Environmental Engineering and Management Journal *June 2018, Vol.17, No. 6, 1417-1424*
http://www.eemj.icpm.tuiasi.ro/; http://www.eemj.eu

"Gheorghe Asachi" Technical University of Iasi, Romania

STUDY OF THE DEVOLATILIZATION KINETICS OF KENAF BY ISOCONVERSIONAL METHODS. INFLUENCE OF VARIABLES

Silvia Román[1*], Beatriz Ledesma[1], Andrés Álvarez-Murillo[1], Awf Al-Kassir[2], Juan Félix González[1]

[1]Department of Applied Physics,
[2]Department of Mechanics, Energetic and Materials,
University of Extremadura, Avenida de Elvas s/n, Badajoz 06006, Spain

Abstract

The thermal degradation of kenaf (*Hibiscus cannabinus*) under the effect of several variables (particle size, Ar flow rate, sample initial mass and heating rate) was investigated. From experimental data and by application of various model-free methods (Friedman, Kissinger-Akahira-Sunose and Flynn-Wall-Ozawa), the activation energies (E_A) were calculated as a function of conversion. The results obtained allowed to conclude that kenaf follows a multi-stage degradation mechanism, with E_A values ranging 170-225 kJ mol^{-1}. Despite the slight differences showed by the three methods on the E_A values, they agreed about the pattern of E_A with conversion.

Key words: kenaf, pyrolysis, kinetics, model-free methods

Received: May, 2013; Revised final: August, 2014; Accepted: August, 2014; Published in final edited form: June 2018

1. Introduction

The environmental effects associated to fossil fuels exploitation, as well as other important issue such as energy dependence or the finite nature of theses fossil resources, make mandatory the shift of current energy scenery towards an increasing contribution of sustainable sources of energy. Among the several renewable energy sources, biomass stands out due to their zero net carbon dioxide emissions and the fact that it allows increasing employment in rural areas (Kucerova et al., 2016; Obernberger, 1998).

The feasibility of using agricultural by-products as renewable energy source by means of pyrolysis and gasification processes has been widely reported. However, the knowledge of the variables affecting the thermal decomposition taking place during these processes is fundamental in order to guarantee an efficient design of the systems and operating conditions. The operating conditions such as decomposition temperature, heating rate, particle size and presence of catalysts, strongly influence the biomass thermal decomposition (Hu et al., 2007; Rusei et al., 2016; Van de Velden et al., 2010).

Kenaf plant (*Hibiscus cannabinus*), native to southern Asia, has arisen great interest due to its fast-growing characteristics and good isolation and mechanical properties. Moreover, kenaf has demonstrated to be very resistant to plagues, which allows the use of very few quantities of fertilizers, which is environmentally and economically advantageous. Due to these characteristics, the use of this plant is growing worldwide and is nowadays higher than 2.6 million tons (Liu, 2000). Moreover, these features make this plant to be considered as a carbon sequestration system, becoming a hot topic for research. However, studies on its characteristics lack, and in particular, and to the best of the authors´ known, there are no pieces of research on their thermal decomposition.

* Author to whom all correspondence should be addressed: sroman@unex.es, Tel.: +34 924289600, Fax: +34 924289601

In this work, the thermal decomposition of kenaf using Ar as inert gas was studied in different experimental series in order to study the influence of the variables: particle size, Ar flow rate, initial sample mass and heating rate. The proper analysis of kinetics involved in these processes can be made by different approaches, as described below.

2. Kinetic study by isoconversional methods. Theoretical consideration

The mathematical approach of the isoconversional methods used in this study is described below. Unlike model-fitting methods, isoconversional ones do not involve any previous assumptions on the reaction mechanisms (Chutia et al., 2013; Khawam and Flanagan, 2005; Vyazovkin and Wight, 1999). Isoconversional methods consider that the reaction rate for a constant extent of conversion is a function of the temperature and the reaction mechanism is independent of the heating rate (Simon, 2004). The fundamental rate equation used in all kinetics studies is generally described assuming that the rates of conversion are proportional to the concentration of reacted material (Eq. 1):

$$\frac{d\alpha}{dt} = k(T)\, f(\alpha) \tag{1}$$

where $k(T)$ is the rate constant and $f(\alpha)$ is the reaction model, a function depending on the actual reaction mechanism.

Eq. (1) expresses the rate of conversion, $d\alpha/dt$, as a function of the reactant mass and rate constant at a given temperature. In this study, the conversion rate α is defined as the relationship between the amount of material reacted at any time and the initial sample mass (Eq. 2):

$$\alpha = \frac{w_o - w_t}{w_o} \tag{2}$$

where w_0, and w_t denote the weight of the sample at initial time (w_0) and at any time (w_t).

The rate constant k is generally given by the Arrhenius equation (3):

$$k(T) = A\exp(-E/RT) \tag{3}$$

where E is the apparent activation energy (kJ mol^{-1}), R is the ideal gas constant (8.314 J mol^{-1}K^{-1}), A is the pre-exponential factor (min^{-1}), and T is the absolute temperature (K).

The combination of Eqs. (1) and (3) yields Eq. (4):

$$\frac{d\alpha}{dt} = A\exp(-E/RT)\, f(\alpha) \tag{4}$$

For a dynamic TGA process, introducing the heating rate, $\beta = dT/dt$, into Eq. (4) gives Eq. (5):

$$\frac{d\alpha}{dT} = \frac{A}{\beta}\exp(-E/RT)\, f(\alpha) \tag{5}$$

Based on this approach, different methods have been proposed as it is subsequently described.

2.1. Friedman method (FR)

Based on Eq. (5), Friedman differential method uses Eq. (6) to determine the kinetic parameters without needing a mathematical model (Friedman, 1964):

$$\ln\left(\frac{d\alpha}{dt}\right) = \ln A + \ln f(\alpha) - \frac{E}{RT} \tag{6}$$

By plotting $\ln(d\alpha/dt)$ vs $(1/T)$ curves at several heating rates, for a constant α, we can get a linear fit whose intercept and slope can be used to calculate the activation energy value, E.

2.2. Flynn-Wall-Ozawa-(FWO) method

This approach is an integral method which is also independent of the degradation mechanism. It involves the measurement of the temperature T, corresponding to a fixed value of conversion degree α, at different heating rates β. By using Doyle´s approximation this method provides Eq. (7) (Ozawa, 1965):

$$\ln(\beta) = -1.0516\frac{E}{RT} + cons \tag{7}$$

The plot of ln β vs $1/T$ provides the slope -1.0516E/R from which the activation energy is obtained. If the determined activation energy is the same for the various values of α, the existence of a single-step reaction can be assumed with certainty. Dissimilarly, a change of E for increasing conversion values suggests a complex reaction mechanism, which invalidates the separation of variables involved in the FWO analysis.

2.3. Kissinger-Akahira-Susone (KAS) method.

This method is based on the expression (8) (Kissinger, 1957; Akahira and Sunose, 1971):

$$\ln\left(\frac{\beta}{T^2}\right) = \ln\left(\frac{AR}{E}\right)\left(-\frac{E}{RT}\right) \tag{8}$$

which is obtained from Coats-Redfern approximation. By plotting $\ln(\beta/T^2)$ vs $1/T$ for constant conversion values (α), the activation energy value (E) can be obtained.

In this work, the thermal degradation of kenaf under different conditions was studied and the devolatilization kinetics was determined, using three different isoconversional methods: Friedman, Kissinger-Akahira-Sunose and Flynn-Wall-Ozawa.

From the experimental data, the values of the activation energy as a function of the extent of conversion were determined.

3. Experimental

3.1. Materials

Previous to thermogravimetric analyses, kenaf fibres were crushed, grounded and sieved to the defined particle size. The ultimate analysis was performed using a LECO CHNS 1000 analyzer and the proximate analysis was carried out following the procedure described elsewhere (CEN/TS 335, 2004). With respect to lignocellulosic analysis, it was determined by Van Soest method (Robertson and Van Soest, 1981). Table 1 shows the lignocellulosic, proximate and ultimate analyses of kenaf fibre. As it can be observed, this material presents a low quantity of N, Cl and S, which is advantageous since it minimizes the corrosion problems associated to the acid rain formation. On the other hand, its low ash content and high volatile proportion, typical of lignocellulosic materials, makes it interesting for pyrolysis processes.

The lignocellulosic composition is typical of biomass materials, although a high content in cellulose can be highlighted.

Table 1. Proximate and ultimate analysis of kenaf

Lignocellulosic analysis (%)			
Cellulose		*69.8*	
Hemicellulose		*12.6*	
Lignine		*17.6*	
Ultimate analysis (%)		***Proximate analysis (%)***	
C	55.41	***Fixed carbon***	*12.36*
H	5.16	***Volatiles***	*79.10*
N	0.33	***Ashes***	*2.32*
S	0.03	***Moisture***	*6.22*
Cl	0.05		
O *	39.02		
Molar ratio H/C: 1.11; molar ratio O/C: 0.53; *Empirical formula: $CH_{1.11}O_{0.53}N_{0.0046}S_{0.0002}$.* ** Balanced*			

3.2. Thermogravimetric study

The experiments were carried out on a thermogravimetric analyzer Setaram SETSYS TG-DTA. Samples were heated from ambient temperature to 700 °C under different conditions, with the aim of studying the influence of the following variables:

a) Particle size influence, in the range 0.14-2 mm (Ar flow rate: 100 cm^3min^{-1}, initial sample mass: 5 mg; heating rate: 60 K min^{-1})

b) Ar flow rate, 25-200 cm^3min^{-1} (particle size: 0.5-1.0 mm, initial sample mass: 5 mg; heating rate: 60 K min^{-1})

c) Initial sample mass, 5-21 mg (Ar flow: 100 cm^3min^{-1}, particle size: 0.5-1.0 mm; heating rate: 60 K min^{-1})

d) Heating rate 10-60 K min^{-1} (Ar flow: 100 cm^3min^{-1}, particle size: 0.5-1.0 mm; sample mass: 5 mg)

The experiments were made in three replicates in order to check the reproducibility. The experimental data in this paper corresponds to the mean value of three runs under identical conditions.

4. Results and discussions

4.1. Influence of variables on the thermal decomposition of kenaf

4.1.1. Particle size

Figure 1 shows the TG and DTG (dm/dt) profiles for the runs performed with kenaf in the particle size range 0.14-2 mm.

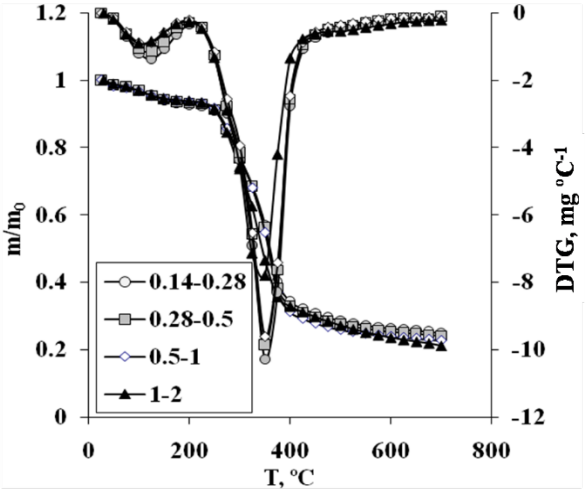

Fig. 1. TG and DTG curves. Effect of particle size. (Ar flow rate = 100 cm^3min^{-1}, Initial sample mass = 5 mg; Heating rate = 60 K min^{-1})

The overlapping of the TG and DTG curves shows that the effect of the particle size in the range studied is very slight. Only the curve of sample 1-2 mm presents a decrease on the intensity of the weight loss in the DTG curve, which could indicate the existence of a certain gradient of temperature for higher size particles. On the other hand, different DTG peaks can be found from Fig 1, which are related to the composition of this material (hemicellulose, cellulose and lignin) (Ulloa et al., 2009; Zabaniotou et al., 2008). The first weight loss in the range 100-180 ºC can be associated to the loss of water present in the material and external water bounded by surface tension (Aboulkas et al., 2009) (DTG peak maxima around 130 ºC). In the DTG plots, it can also be observed that this peak is steeper as the particle size is decreased. This is turn indicates that the drying of this material is faster for lower particle sizes, as the surface available to heat interchange is higher.

The peak found around 350 ºC corresponds to the decomposition of light volatiles; this step is often related to the degradation of hemicellulose and cellulose (Fang et al., 2006; Li et al., 2004). Li et al. have found that the pyrolysis of hemicellulose is completed at around 350 ºC, while that of cellulose is accomplished in the range 250-500 ºC (Li et al., 2004).

As a consequence, a shoulder on the left-side of cellulose peak appears around 225 ºC for samples with a high content in hemicellulose. As inferred from Figure 1, this is not the case of our material, whose hemicellulose content is low if compared to that of cellulose (Table 1).

Lignin, which is representative of the heaviest volatiles, is more thermally stable, and its decomposition range is wide (150-900 ºC), usually overlapping with those of hemicellulose and cellulose. In this way, no visual signal such as a peak can be identified for lignin in the DTG curve (Aboulkas et al., 2009; Friedl, 2012; Li et al., 2004).

The runs were made in non-isothermal regime in order to determine if the mass and energy transport processes affect the velocity of the pyrolysis process and to identify the range of operating conditions under which the chemical reaction is the controlling step, since only under these conditions the velocity can be used to calculate the pyrolysis kinetics. There are three transport mechanisms which can influence the global process kinetics:

- intraparticular transport, which is affected by the particle size
- particle-fluid transport, which depends on the inert gas flow and the particle size
- interparticular transport, which depends on the number of sheets in the crucible where the sample is placed.

For a fixed particle size and crucible, the intraparticle transport can be studied by varying the initial sample mass (Galam and Smith, 1983). Once this variable has been optimized, the study of the remaining variables can be made.

Our results indicate that the use of different particle sizes up to 1 mm does not exert any appreciable effect on the process velocity. However, an increase of this variable in the range 1-2 mm and presumably for higher values of particle size causes a rise in the temperature gradient of the inner of the particle, thus adding a contribution to the process kinetics. For this reason, in order to ensure a negligible contribution of intraparticular transport and particle-fluid transport, a particle size of 0.5-1 mm was chosen for the subsequent stages of this study.

4.1.2. Argon flow rate

During pyrolysis processes, the flow rate of inert agent affects the residence time of the gases produced. Thus, a high flow minimizes the occurrence of secondary reactions between gaseous products themselves (cracking reactions) and also the existence of reactions between some oxidant products (such as hydrogen or carbon dioxide) and the gas or the char.

Figure 2 shows the TG and DTG curves corresponding to this experimental series. From the overlapping of both types of curves, it can be infered that increasing the flow rate has a scarce influence on kenaf thermal decomposition. This effect has also been found during the pyrolysis of cherry stones (González et al., 2003). A flow rate of 100 cm^3min^{-1} was chosen for making the subsequent runs.

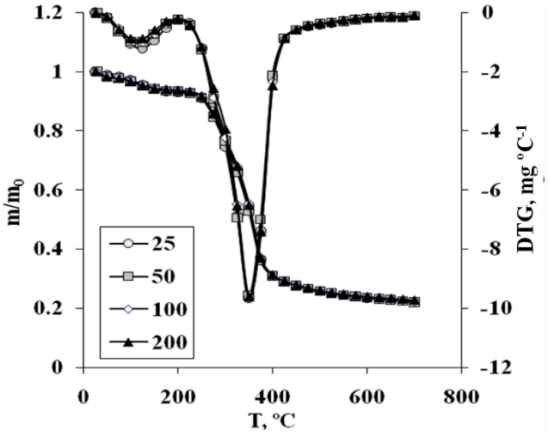

Fig. 2. TG and DTG curves. Effect of Ar flow rate. (Particle size = 0.5-1.0 mm, Initial sample mass = 5 mg; Heating rate = 60 K min^{-1})

4.1.3. Initial sample mass

This study was made using the following conditions: particle size of 0.5-1 mm, Ar flow rate of 100 cm^3min^{-1} and heating rate of 60 K min^{-1}. Under these conditions, the influence of the initial sample mass was studied in the range 5-21 mg. Figure 3 shows the TG and DTG curves for these series. As inferred from the TG curves, the normalized weight loss is almost identical in all cases. For DTG curves, the intensity of the decomposition is evidently larger as the initial mass is increased.

In relation with the temperature associated to each characteristic peak, no variation was found for the different runs, as it has been pointed out in other works who investigated this effect with other precursors (González et al., 2003). Besides, according to work done by Galam and Smith, we ensure that we do not overcome of two to three layers of particles placed in the weighing basket below 5 mg, then results showed that transport of heat and mass were not influenced. Since no significant differences were found between the range of particle size studied, a sample mass of 5 mg was used in subsequent runs.

4.1.4. Heating rate

4.1.4.1. TGA analyses

This variable was studied in the range 10-60 K min^{-1}, using a particle size of 0.5-1 mm, Ar flow rate of 100 cm^3min^{-1} and an initial sample mass of 5 mg. Under these conditions the process is controlled mainly by the chemical kinetics and the limitations of mass and energy transfer are minimized.

Figure 4 shows the TG and DTG curves corresponding to this experimental series. As it can be observed, a higher heating rate causes a shift of the temperature at which the characteristic peaks are observed to higher values. Also the slope of the TG curve gets greater as the heating rate decreases. This trend is usually found for non-isothermal experiments (Wang et al., 2008; Min et el., 2007) and can be related to the fact that using lower heating rates can favour the intraparticular energy transfer, since the reaction time is longer.

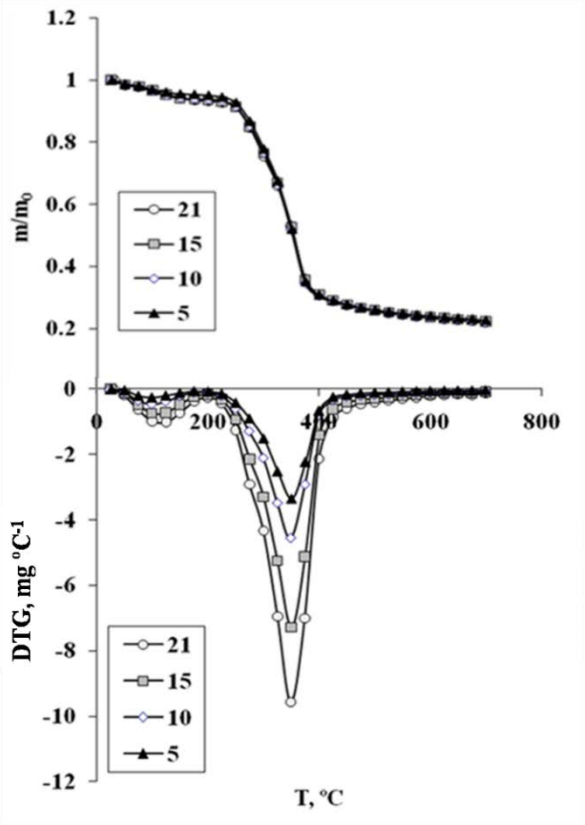

Fig. 3. TG and DTG curves. Effect of initial sample mass (Ar flow rate = 100 cm^3min^{-1}, Particle size = 0.5-1.0 mm; Heating rate = 60 K min^{-1})

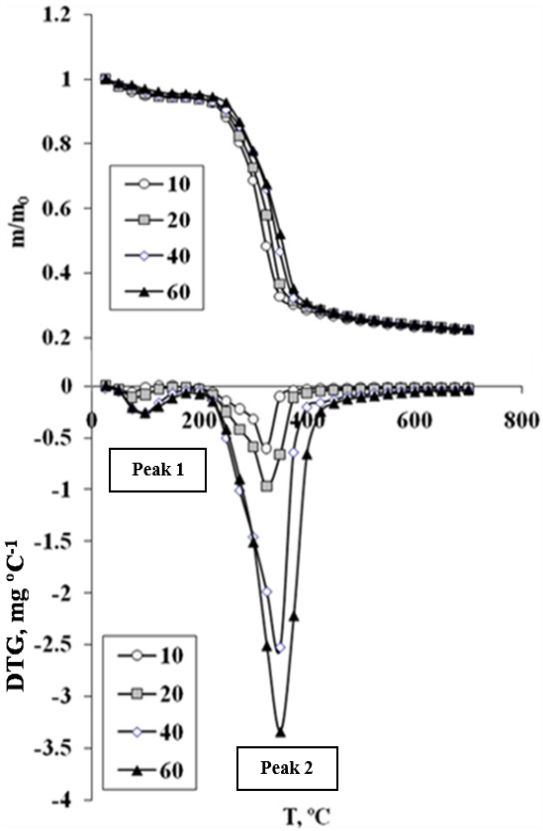

Fig. 4. TG and DTG curves. Effect of heating rate. (Ar flow = 100 cm^3min^{-1}; Particle size = 0.5-1.0 mm; Sample mass = 5 mg)

The overall effect causes a lower kinetics and thus a delayed decomposition (Wang et al., 2008). Another possible explanation can be related to the fact that increasing the heating rate can influence the secondary reactions between the char and the products of primary pyrolysis such as tars and high molecular weight compounds. In Table 2 some pyrolysis characteristics parameters have been collected for the different heating rates studied. These parameters are T_i (temperature at which peak 2 starts), T_{max} (temperature of peak 2 maximun), $(dw/dt)_{max}$ (maximum degradation rate) and VM (total volatile matter).

As it can be seen, increasing the heating rate causes a shift of T_i and T_{max} towards higher temperatures, and the maximum degradation rate gets steeper. On the other hand, the percentage of sample removed is almost constant in the four experiments made in this series; that is to say, a higher temperature is needed for achieving a given weight loss, when the heating rate is increased. This fact will be discussed in detail with the aid of DTA analyses, shown in next section.

4.1.4.2. DTA analyses

Figure 5 shows the DTA curves for this experimental series. As it can be observed, three peaks can be found: the first and second one correspond to the temperatures related to the first and second peaks of the DTG curves (Fig. 4), while the third peak is located at 450 ºC. Moreover, there is a clear effect of the heating rate on the heat transference; as this variable increases, the endothermal peaks get larger.

Making a correlation between DTA peaks and particular decomposition events is a really complex task, given the heterogeneity of biomass. Some previous pieces of research state that hemicellulose decomposes exothermally around 200 ºC in nitrogen (Gaur and Reed, 1995). Also, cellulose decomposition has been related with an endotherm commencing around 290 ºC, although sometimes an exotherm is found around 350 ºC. Finally, lignin is associated to a flat exothermic peak commencing at 300 ºC and reaching a maximum at 425 ºC.

Table 2. Characteristic parameters during pyrolysis at various heating rates

HR ***(K min^{-1})***	***T_i*** ***(ºC)***	***T_{max}*** ***(ºC)***	***$(DTG)_{max}$*** ***(mg min^{-1})***	***VM*** ***(%)***
10	175	325	7.24	62
20	200	325	14.43	63
40	200	350	27.20	64
60	201	351	38.80	64

From Fig. 5, it can be noted that at temperatures close or greater that 200 ºC DTA signal starts increasing, and two clear positive peaks are found around 350 and 475 ºC. A negative peak is located near 400 - 425 ºC, and then, at the end of the process, the signal intensity decreases. From our results, it is obvious that these events overlap and, as previously stated, their identification is not straightforward. We could just suggest that the intermediate peak might (400 - 425 ºC) be related to cellulose endothermal decomposition, while the signal at 350 ºC could be associated to delayed exothermal hemicelluloses degradation. Lignin decomposition might be occurring from the beginning of the process up to the end, and therefore its exotherm would overlap with the previous ones, also being observed as a decreasing signal at the end of the process.

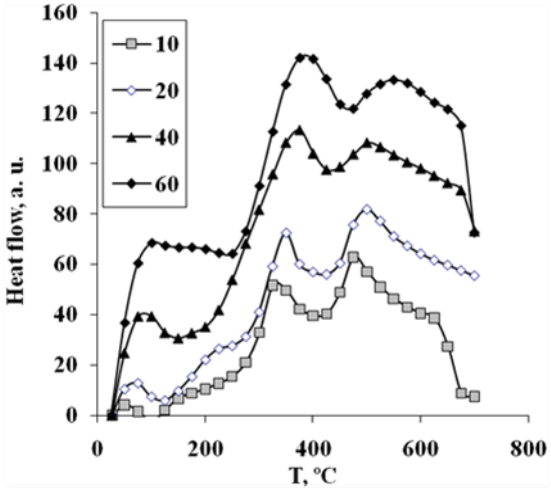

Fig. 5. DTA curves. Effect of heating rate (Ar flow = 100 cm^3min^{-1}; Particle size = 0.5-1.0 mm; Sample mass = 5 mg)

The values of temperature corresponding to these three peaks are shown in Table 3: T_I corresponds to the first one, T_{II} to the second one and T_{III} for the third one. From this Table one can deduce that higher heating rates causes a shift of these peaks to higher values of temperature, in coherence with DTG profiles. These effects can be related to the fact that using a greater heating rate decreases the time that the gas products permanence in the crucible, and in consequence, the chance of occurrence of secondary reactions between these gases and the biomass residue. With a minor presence of oxidant gases to react with the char, a greater temperature might be necessary to reach a given carbon conversion.

4.2. Kinetic analysis

The experimental data of the thermal degradation of Kenaf under different heating rates (10, 20, 40 and 60 °C min^{-1}) were used for the determination of the kinetic parameters. For this task, the use of isoconversional methods allowed to relate the activation energy (E) to the conversion (α) without previous assumptions on the reaction mechanism model. As it has already been inferred from the thermogravimetric curves in section 3.1, the thermal degradation of kenaf seems to occur at different rates depending on the range of temperature considered. Thus, at first glance, it could not be concluded that the decomposition of this material is a single-step process.

Table 3. Characteristic values of Temperature in DTA curves at various heating rates (HR)

HR (K min^{-1})	T_I (ºC)	T_{II} (ºC)	T_{III} (ºC)
10	50.64	325.19	475.03
20	75.01	350.26	500.11
40	100.49	375.42	500.39
60	100.52	400.37	549.94

The plots corresponding to the fitting of isoconversional Friedman, FWO and KAS methods are shown in Figs. 6, 7 and 8, respectively. In these figures, the dependence of the activation energy on the conversion in the range 0.2-0.8, according to the isoconversional methods, can be observed.

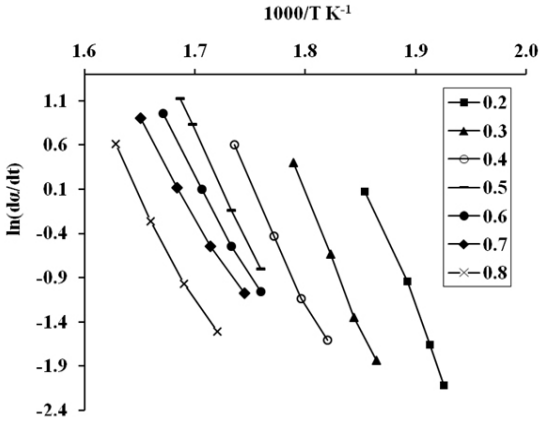

Fig. 6. Iso-conversional plot according to Friedmann method for different α values

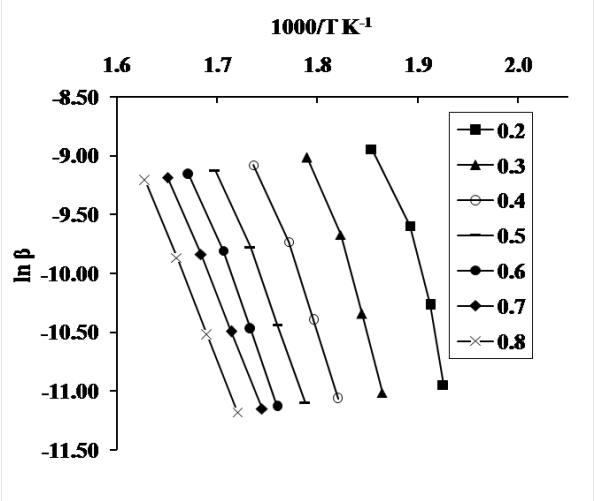

Fig. 7. Iso-conversional plot according to F-W-O method for different α values

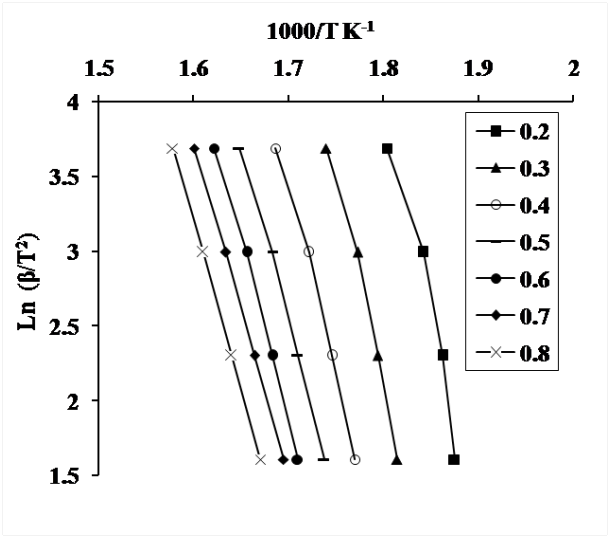

Fig. 8. Iso-conversional plot according to K-A-S method for different α values

The straight lines joining the model data are nearly parallel, especially for Friedman and FWO models, although some remarks can be made. Aboulkas et al. have obtained a similar tendency for olive waste, also finding a greater separation of the curves themselves for lower conversions (Aboulkas et al., 2009). The parallel between the lines can be related with the reaction mechanism. The more parallel they are, the greater probability of being a single reaction mechanism.

The differences in the reaction mechanisms for particular conversion values might be caused by the complex reactions in the decomposition process of the main components according to previous research; that is to say, the parallel is a function of the conversion, and its variations can be associated to changes of the different chemical compositions of the natural fiber of kenaf (Mohanty et al., 2000). As previously described, the contribution of the cellulose and hemicellulose degradation to the overall decomposition scheme is greater at values of conversion lower than 0.5. This effect can be observed in Figs. 7-8, where the parallel of the isoconversional lines is slightly affected at lower α.

The relation between the activation energy and the conversion values, based on the three isoconversional methods, has been plotted in Fig. 9. As it can be seen, some variations are observed at the very initial and final stages, providing E_a values in the range 180-255 kJ mol^{-1}. The application of Friedman, KAS and FWO models to the experimental data gave average values of activation energy of 215.34, 194.53 and 204.27 kJ mol^{-1}, respectively.

The fact that the apparent activation energies obtained by Friedmann method are higher than those obtained by FWO and KAS methods might be due to the fact FWO and KAS methods involve a systematic error in activation energy that does not appear in the FR method; while the differential method (FR) uses the point value of the overall reaction rate, the integral methods (KAS and FWO) describe the history of the system by integration (Vyazovkin, 2001).

Independently of the calculation procedure used, the activation energy presents a similar tendency in the 0.2-0.8 conversion range. As inferred from Fig. 9 the activation energy obtained from the Friedman method varies up to conversion values of 60%, while for higher values (temperatures above 350°C), the activation energy remains relatively stable with a value around 220 kJ mol^{-1}. This value is in all cases greater for higher conversion values.

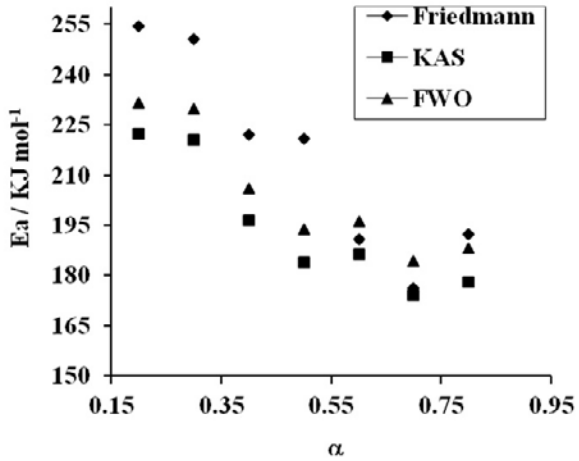

Fig. 9. Comparison of apparent activation energy (E) as a function of conversion (α) by Friedman, FWO and KAS models

Also, when the conversion rate exceeds 60%, the calculation errors increase, which in turn could be indicative to a change in the reaction mechanism. These results confirm that kenaf degradation cannot be considered as a single step process, but it proceeds via different stages.

5. Conclusions

The study of the thermal degradation of kenaf under the effect of various experimental conditions allowed obtaining the following conclusions:

a) Increasing particle size causes a certain gradient of temperature which slows the thermal degradation process for particles sized 1-2 mm.

b) The influence of Ar flow rate on the pyrolysis process, under the range studied is scant.

c) The initial sample mass slightly influences the temperature at which the characteristics weight losses are produced.

d) Increasing the heating rate has a clear effect on the thermal degradation process, which might be associated to the existence of a temperature gradient due to shorter reaction times.

e) The kinetics of the thermal degradation of kenaf was studied by isoconversional methods (Friedman, KAS and FWO) regarding the reaction mechanism. The activation energy obtained in the 0.2-0.8 conversion range presents differences depending on the isoconversional method used.

Also, it could be concluded that the pyrolysis of kenaf cannot be considered as a single step process, but it proceeds via different stages.

References

Aboulkas A., El harfi K., El Bouadili A., Nadifiyine M., Benchanaa M., Mokhlisse A., (2009), Pyrolysis kinetics of olive residue/plastic mixtures by non-isothermal thermogravimetry, *Fuel Processing Technology*, **90**, 722-728.

Akahira T., Sunose T., (1971), Trans. Joint Convention of Four Electrical Institutes, Paper No. 246, Research Report, **16**, 22–31.

CEN/TS 335 (2004) Biomass standards, Technical Specifications CEN/TS-Solid Biofuels, On line at: https://www.sis.se/api/document/preview/36149/.

Chutia R.S., Kataki R., Bhaskar T., (2013) Thermogravimetric and decomposition kinetic studies of Mesua ferrea L. deoiled cake, *Bioresource Technology*, **139**, 66-72.

Fang M.X., Shen D.K., Li Y.X., Yu C.J., Luo Z.Y., Cen K.F., (2006), Kinetic study on pyrolysis and combustion of wood under different oxygen concentration by using TG-FTIR analysis, *Journal of Analytical and Applied Pyrolysis*, **22**, 7-77.

Friedl A., (2012), Lignocellulosic biorefinery, *Environmental Engineering and Management Journal*, **11**, 75-79.

Friedman H., (1964), Kinetics of thermal degradation of char-forming plastics from thermogravimetry. Application to a phenolic plastic, *Journal of Polymer Science, Part.* **C6**, 183-195.

Galam M.A., Smith J.M., (1983), Pyrolysis of oil shale: experimental study of transport effects, *American Institute of Chemical Engineers Journal*, **29**, 604-610.

Gaur S., Reed T.B., (1995), An atlas of thermal data for biomass and other fuels, National Technical Information System, Springfield, US.

González J.F., Encinar J.M., Canito J.L., Sabio E., Chacón M., (2003), Pyrolysis of cherry stones: energy uses of the different fractions and kinetic study, *Journal of Analytical and Applied Pyrolisis*, **67**, 165-190.

Hu S., Jess A., Xu M., (2007), Kinetic study of Chinese biomass slow pyrolysis: Comparison of different kinetic models, *Fuel*, **86**, 2778-2788.

Khawam A., Flanagan D.R., (2005), Complementary use of model-free and modelistic methods in the analysis of solid-state kinetics, *Journal of Physical Chemistry B*, **109**, 10073-10080.

Kissinger H. E., (1957), Reaction kinetics in differential thermal analysis, *Analytical Chemistry*, **29**, 1702-1706.

Kucerova I., Banout J., Lojka B., Polesny Z., (2016), Performance evaluation of wood-burning cookstoves in rural areas near Pucallpa, Peru, *Environmental Engineering and Management Journal*, **15**, 2421-2428.

Li S., Xu S., Liu S., Yang C., Lu Q., (2004), Fast pyrolysis of biomass in free-fall reactor for hydrogen-rich gas, *Fuel Processing Technology*, **85**, 1201-1211.

Liu A., (2000) *World Production and Potential Utilization of Jute, Kenaf, and Allied Fibers*, Proc. of the 2000 International Kenaf Symposium, Hiroshima, 13–14 October, Japan.

Min F., Zhang M., Chen Q., (2007), Non-isothermal kinetics of pyrolysis of three kinds of fresh biomass, *Mining Technology*, **17**, 105-111.

Mohanty A.K., Misra M., Hinrichsen G., (2000), Biofibre, biodegradable polymers and biocomposites: an overview, *Macromolecular Materials and Engineering*, **1**, 276-277.

Obernberger I., (1998), Decentralized biomass combustion: state of the art and future development, *Biomass and Bioenergy*, **14**, 33-56.

Ozawa T., (1965), A new method of analyzing thermogravimetric data, *Chemical Society of Japan*, **38**, 1881-1886.

Robertson J. B., Van Soest P. J., (1981), *The Analysis of Dietary Fibre in Food*, Marcel Dekker, New York.

Rusei A.C., Stefanescu I., Ifrim I., (2016), Effects of different pretreatments on biomass composition evaluated by spectral and chemometric techniques, *Environmental Engineering and Management Journal*, **15**, 635-644.

Simon P., (2004), Isoconversional methods: fundamentals, meaning and application, *Journal of Thermal Analysis and Calorimetry*, **76**, 123-132.

Ulloa C.A., Gordon A.L., García X.A., (2009), Thermogravimetric study of interactions in the pyrolysis of blends of coal with radiata pine sawdust, *Fuel Processing Technology*, **90**, 583-590.

Van de Velden M., Baeyens J., Brems A., Janssens B., Dewil R., (2010), Fundamentals, kinetics and endothermicity of the biomass pyrolysis reaction, *Renewable Energy*, **232**, 42-35.

Van Soest P.J, Wine R.H., (1968), Determination of lignin and cellulose in acid-detergent fiber with permanganate, *Journal Association of Official Analytical Chemists*, **51**, 780-785.

Vyazovkin S., Wight C.A., (1999), Model-free and model-fitting approaches to kinetic analysis of isothermal and nonisothermal data, *Thermochimica Acta*, **340/341**, 53-68.

Vyazovkin S., (2001), Modification of the integral isoconversional method to account for variation in the activation energy, *Journal of Computational Chemistry*, **22**, 178-183.

Wang G., Li W., Li B., Chen H., (2008), TG study on pyrolysis of biomass and its three components under syngas, *Fuel*, **87**, 552-58.

Zabaniotou A., Ionannidou O., Antonakou E., Lappas A., (2008), Experimental study of pyrolysis for potential energy, hydrogen and carbon material production from lignocellulosic biomass, *International Journal of Hydrogen Energy*, **2433**, 44-33.